- Technical Paper -

EFFECTS OF STEEL FIBERS ON SHEAR STRENGTH AND DEFORMATION BEHAVIOR IN SHORT SFRC BEAMS WITHOUT STIRRUPS BY FULL FIELD OPTICAL ESPI AND FEM METHODS

Timothy NYOMBOI[*1], Hiroshi MATSUDA[*2], Yukihiro ITO [*3]

ABSTRACT

The potential of utilizing steel fibers as additional or minimum shear reinforcement in RC beams has been reported widely in the literature. Few studies substantiate on the influencing factors contributing to the shear strength enhancement in steel fiber reinforced concrete beams (SFRC). To bridge this gap, this study investigated short SFRC beams under bending-shear by optical full field and Finite Elements analysis methods. It is shown that enhanced crack strain capacity, cracking propagation and ductility contribute significantly to the shear strength and deformation improvement in SFRC beams.

Key words: steel fiber reinforced concrete beam, shear strength, cracking, strain, finite element method, electronic speckle pattern interferometry method

1. INTRODUCTION

Steel fiber reinforced concrete (SFRC) as a modern construction material has been applied in tunnels, wall cladding, industrial slabs, pipe repair, bridge decks, and pavements [1-3]. SFRC possess good energy absorption and impact characteristics and can function well in providing ductility in beam column assembly [4], crack control in slabs, beams as well as pre-cast elements [5]. Many reports published in the past two and half decades have considered the possibility of utilizing steel fibers as shear reinforcements in structural elements [6].

Shear behavior in SFRC beams has been investigated experimentally by a number of researchers [7, 9, 16-21]. However, limitation of the conventional measurement methods applied in these studies hinders the full potential of quantifying and understanding the behavior [8]. Random and discrete presence of steel fibers in the concrete volume of the beam in contrast to conventional reinforcements (stirrups and re-bars) is expected to effect more on strain capacity, cracking propagation and ductility characteristics. These properties influence the shear load carrying capacity in SFRC beams. Moreover, few attempts have been made in the past to numerically simulate the response of steel fiber reinforced elements [9]. According to Feheling [9], lack of suitable constitutive material models for SFRC composite is a contributing factor. Developing material models for SFRC is relatively a very complex task because of the different geometric scales involved in the initiation and propagation of damage leading to failure [9].

In this study, an attempt is also made to numerically simulate the shear behavior in the SFRC beams by applying an experimental SFRC stress strain material model [8]. Strain based models are attractive, since there is no need for abstract sophisticated crack laws, furthermore stress strain relations can be input directly [10] and the terms used are familiar with structural engineers dealing with traditional design of concrete structures[11].

On the other hand non contact full field optical ESPI method can be used to evaluate the deformation characteristics in detail. Results can be used to directly validate similar results from the FEM model analysis. Matsuda et al, [12] have dealt in detail on basic principles and the effectiveness of the method in an RC structure has been confirmed [9, 12, 13].

Therefore, the objective of the present study is to examine and clarify the influence of steel fibers on shear behavior in short SFRC beams by applying full field optical Electronic Speckle Pattern Interferometry (ESPI) and Finite Element analysis methods. Load deflections, cracking generation, propagations, stress and strain distribution behavior is examined.

2. Experimental programme

2.1 Materials and casting

Four variable concrete mix proportions were made as shown in Table1. Standard ordinary Portland cement and normal aggregates meeting the JSCE guidelines for concrete [14] were used. Workability of the mix was improved by using a water reducing admixture (0.8% content by volume) without increasing the water content. The 28day average cylinder compressive strength of the concrete was 38MPa. End hooked discrete steel fibers with an aspect ratio of 48.4 (Fig.1) were mixed with the concrete in fresh state before casting. Further, the beams were reinforced in

*1 Graduate School of Science and Technology, Nagasaki University, M.Phil. Eng, JCI Member
*2 Prof., Dept. of Structural Engineering, Nagasaki University, Dr. Eng., JCI Member
*3 Associate. Prof, Dept. of Civil Engineering, Saga University, Dr. Eng., JCI Member

Fig.1 Collated end hooked steel fiber

Table 1 Concrete mix proportions

Fiber %	Kg/m^3				
	Water	Cement	Gravel	Sand	Admix. (AE)
0	171	377	938	712	3
0.5	171	377	930	707	3
1	171	377	923	700	3
1.5	171	377	916	695	3

Table 2 Characteristics of Reinforcement

Type	Diameter (mm)	Elastic Modulus (GPa)	Tensile strength (MPa)	Remark
fiber	0.62	210	1000	hooked
Bar	6	210	340	deformed

flexure with 6mm diameter deformed re-bars. The properties of these reinforcements are given in Table 2.

2.2 Specimens and Test procedure

Eight 400x100x100mm simply supported short beams with no stirrup reinforcements were tested in bending-shear, under a variable shear span to depth ratio (a/d) of 1 and 1.5 (full details shown on Fig.2). To distinguish the influence of the steel fibers on shear strength from the expected shear reserve strength (compression shear failure effect), particularly in the beams with shear span to depth ratio a/d=1, all beams including the control beams (no fiber) were ensured that they are of the same geometry with same flexural reinforcements. Only steel fiber content and the shear span to effective depth ratio (a/d) were varied. Controlled loading was applied using a 300kN Universal testing machine. Deformations were monitored and recorded using a set of optical ESPI equipment consisting of a desk top computer (PC), and CCD camera equipped with laser beam sensors (ESPI sensor) as shown in Fig.3. Target areas of ESPI measurement (Fig.2a) were sprayed with special white (UNI Glo) paint to create a reflective surface in order to obtain a better contrast in the captured images during deformation. For graphical illustrations, shear strains were obtained from ESPI shear strain full field results at point 1(Fig.2b). In addition, crack strain distribution behavior was evaluated along the location indicated by the line A-A as shown in Fig.2b. Displacement at various load states were also obtained at point 2 (Fig.2b) from ESPI displacement full field results. ISTRA ESPI programs were used to record, control and evaluate the speckle interferograms resulting from the deformation of the specimens. Control and recording of the loads were performed using a data logger and a laptop PC. From the recorded load history average shear stresses were computed for each load state corresponding to the full field deformation state (from ESPI).

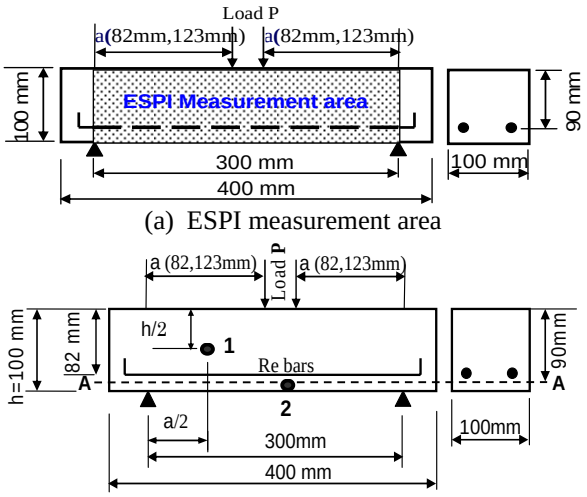

Fig.2 Test RC beam set up and measurement locations

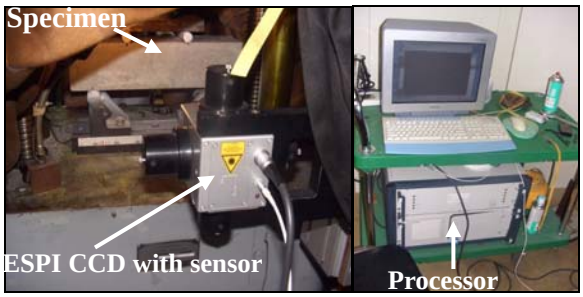

Fig.3. Full field optical equipment and set up

3. NUMERICAL INVESTIGATION

3.1 FE Analysis

In the numerical study, SOFISTIK FEM code [15] was used. Modeling and analysis was programmed using SOFISTIK CADINP language. Incremental loading and modified Newton Raphson method was applied in the analysis. Speed and convergence is increased through Crisfield accelerating algorithm. This method notices the residual forces developing during the iterations and calculates the Crisfield coefficients applied in which convergence is determined. In the iteration steps, new displacements and stresses are determined. It is checked whether cracks or any other non-linear effects have occurred at any element. Cracked elements are considered with a reduced stiffness.

(1) Structural model

Fig.4 shows the two dimensional meshed RC beam. The model was designed to replicate the test specimens. Four node quadrilateral isoparametric plane stress elements were used to model the SFRC/plain concrete elements. In plane elements of SOFISTIK, a general quadrilateral element with four nodes (QUAD) is sufficient, so that the introduction of the six-to nine-noded isoparametric elements is not necessary [15].

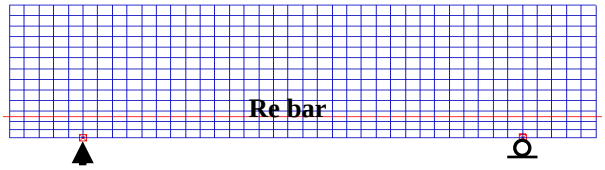

Fig. 4 Meshed RC beam model

(2) Material model

It has been established that steel fibers do not significantly influence the strength in compression but rather in tension [1, 8, and 16]. Based on this finding, variable non linear stress-strain relation in tension was defined and an average non linear stress-strain relation in compression was applied as reported elsewhere by the authors [8]. The variable material model in tension corresponds to the variable fiber content used (0% to 1.5% content by volume). The variability is occasioned by the different strength-strain capacities attributed to the variable steel fiber content in the concrete. The tension material model profile consist of a linear part up to yielding, a non linear part up to ultimate level which is characterized by a increase in strength (in fiber concrete) and a softening part characterized by a reduction in strength and an increasing strain particularly in the case of the higher fiber content (e.g. 1.5%). These material models were assumed to be sufficient for both fiber and non fibrous concrete in the numerical study. Material behavior for the reinforcing bars was defined with a standard elastic-perfect plastic stress strain relation. The flexural reinforcement (re-bars) properties were same as those used in the tests.

4. RESULTS AND DISCUSSION

The results are presented in form of strength curves, cracking and strain distribution plots. For ease of presentations and discussions, specimens are designated according to the volume percentage of steel fibers used. These designations which are used in the subsequent sections are as follows:

FB0.5 to FB1.5%: *Fiber beams (fiber content)*
CB0% : *Control beam (non fibre)*

4.1 Cracking pattern

Fig.5 and Fig.6 depicts the shear-flexural failure modes observed from experiments and the numerical (FEM) analysis. It is observed that at ultimate load state, optical ESPI result depicts more cracks that could not be easily observed with the naked eye. This is apparent in the fibrous beams FB1.5%, shown in Fig.5b and 6b. In the opinion of the authors this behavior indicates increased cracking propagation in SFRC beams due to the stress re-distribution efficacy of the steel fibers. This behavior is confirmed further by the increase in crack strain capacity and distribution (Fig.13 and 15). Generally, the physical cracking pattern for each category (fibrous and non fibrous beams) compares fairly well with the experimental results. The numerical results (Fig.5c and 6c) shows that in CB0% beam (in a/d=1 group), cracks having widths of 0.4mm to 1.4mm were formed, while those in FB1.5% beam range from 0.9 to 3.7mm. In a/d=1.5 group (Fig.6c), cracks range from 0.1mm to 6.6mmm and 0.1 to 1.6mm in the fibrous beam (FB1.5%) and control beam (CB0%), respectively. More flexural cracks are noted in a/d=1.5 group of beams.

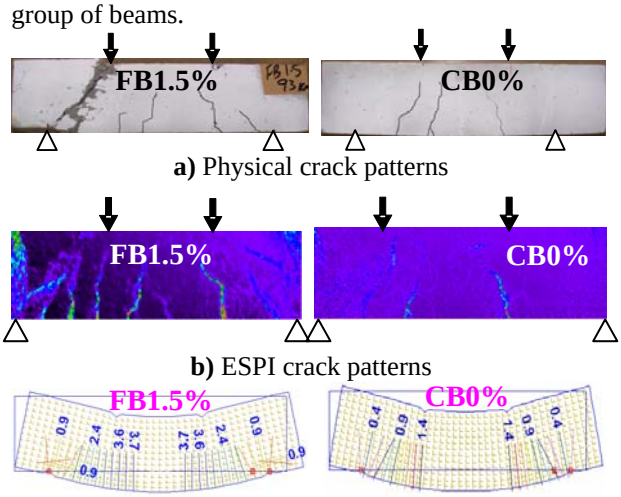

a) Physical crack patterns

b) ESPI crack patterns

c) FEM crack pattern and widths (mm)

Fig. 5 Test and FEM Crack pattern in a/d=1 group of beams (at ultimate load)

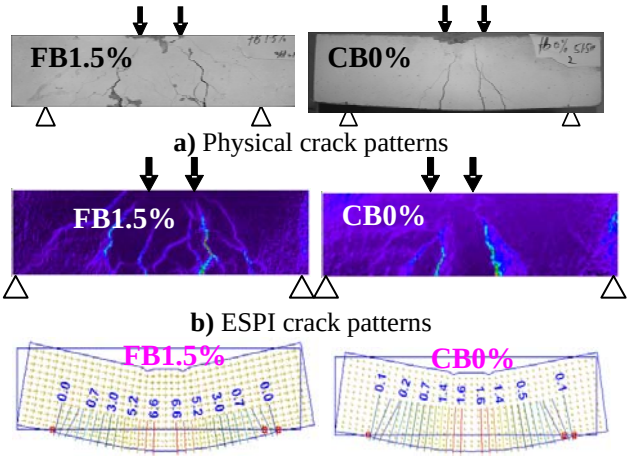

a) Physical crack patterns

b) ESPI crack patterns

c) FEM crack pattern and widths (mm)

Fig. 6 Test and FEM Crack pattern in a/d=1.5 group of beams (at ultimate load)

4.2 Load-deflection response

Figs.7 and 8 shows the test load deflection response and the corresponding FEM results are as shown in Figs.9 and 10. It can be seen that in the initial phases, both the experimental and numerical load deformation response is approximately linear. However beyond the yield point (point of deviation from linearity; approximately at 40kN, 20kN and 60kN, 40kN, in Figs 7, 8 and 9, 10, respectively), non linear behavior occurs in which the influence of the steel fibers after cracking is observed. By comparing control (CB0%) and fibrous (FB0.5% to FB1.5%) load deflection response after cracking (as marked by point of deviation from linearity, see Figs.7 to 10), it is noted that strength in the fibrous beams are higher than those of the control beams. The increase in cracking

propagation (Fig.5b and 6b) and the strain distribution behavior in the fibrous beams (Figs.13 and 15) indicate the deformation enhancement and hence strengthening effect of the steel fibers. Summary of the strength comparisons and increase in SFRC beams are as given in Table 3. In strength increase determination, the base values used are the CB0% ultimate strengths. It is evident from the results (Table 3) that fibrous beams in a/d=1 group had higher strength increase. For example in a/d=1 group, strength increase of 50% is obtained in both experimental and FEM results for FB1.5% while for the same beam type (FB1.5%) in a/d=1.5 group, the increase is 22%. The correlation factors (T/F) given in Table 3 indicates that the FEM ultimate strengths results compare well with the experimental values. Since all the beams had the same flexural reinforcement, geometry (cross sectional and longitudinal) and were tested under the similar set up conditions, it can be concluded that the strength increase in fibrous beams was due to the fibers influence, rather than compression reserve strength, otherwise the ultimate strength results should have been the same for all the beams (with or without fiber).

From deflection point of view (Figs 7 to 10) ductility improvement is noted in the fibrous beams when compared with the control beam (CB0%). Experimental load displacement response for FB1% and 1.5% appear to approach almost the same level after yielding. This may be an indication of the optimum fiber content, beyond which significant effect is minimal. A reduction in strength and increase in deflections with increasing shear span to depth ratio is noted (Fig.7 to 10).

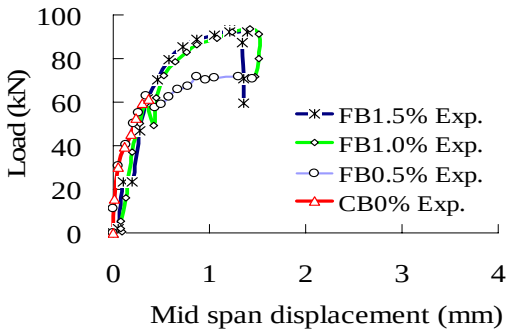

Fig. 7 Test load displacement curves for a/d=1 group of beams

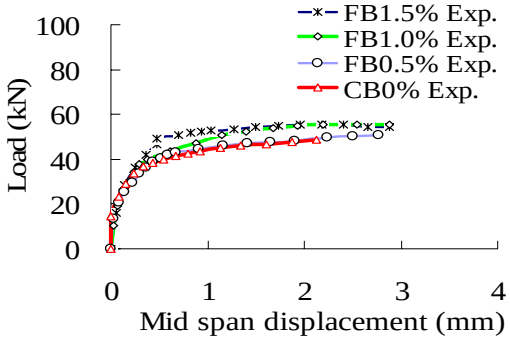

Fig. 8 Test load displacement curves for a/d=1.5 group of beams

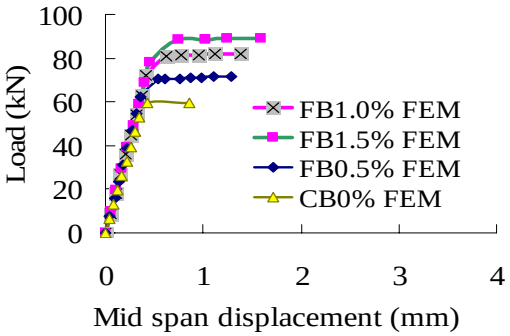

Fig. 9 FEM load displacement curves for a/d =1 group of beams

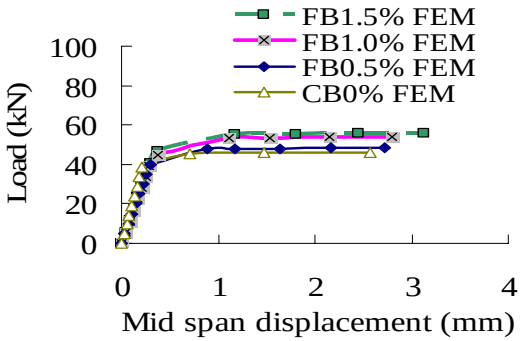

Fig. 10 FEM load displacement curves for a/d=1.5 group of beams

Table 3 Ultimate strength comparisons

a/d	Beam Type	Ultimate Load (kN)			Strength increase %	
		Test (T)	FEM (F)	T/F	Test	FEM
1	**CB0**	62	60	1.03	-	-
	FB0.5	71	72	0.99	15	20
	FB1.0	94	84	1.25	52	40
	FB1.5	93	90	1.03	50	50
1.5						
	CB0	49	46	1.06	-	-
	FB0.5	52	49	1.06	6	7
	FB1.0	55	55	1.00	12	20
	FB1.5	56	56	1.00	22	22

4.3 Shear stress and strain distribution behavior

Fig.11a and b shows the FEM shear stress and strain distribution behavior in a/d=1 beams. Figs.12 and 14 depicts the experimental shear stress strain curves for a/d=1 and 1.5 respectively. Figs.13 and 15 shows the strain distribution behavior in these beams along the indicated location (A-A; see details in Fig.2). From Fig.11, the numerical ultimate shear stress in fibrous (FB1.5%) is approximately 1.5 times that of the control beam (CB0%). These values are 4.7N/mm^2 and 3.1N/mm^2 in FB1.5% and CB0% respectively. It is noted that these values are in agreement with the ultimate experimental shear stress values shown in Fig.12. The predominant effect of steel fibers on the strain behavior after cracking is evident in Fig 13 and Fig.15. Cracking is marked by points with peak strain

concentrations. It can be seen that higher peak crack strains and increased distribution occurs in the fibrous beam (FB1.5%) in comparison with Control beam (CB0%). The maximum strain achieved in the vicinity of a crack in FB1.5% is 0.04 and 0.073 while in the control beams (CB0%) the result is 0.016 and 0.056 in a/d =1 and 1.5 group of beams, respectively (see Figs.13 and 15). These points with maximum crack strains also indicate the positions of the largest crack that occurred in each beam (see Figs 5a and 6a). In a/d=1 group, the average experimental principal strain values (mean of all strain values along line A-A in each beam type) are found to be 0.002 and 0.004 for CB0% and FB1.5%, respectively. These values compare fairly well with the corresponding average FEM principal strain values (mean of all the values in the tension region as given by the positive values shown in the key title of Fig.11b), and are found to be 0.006 and 0.002 for FB1.5% and CB0%, respectively. Generally fibrous beam specimens showed superior deformation behavior which can be attributed to the crack bridging and stress redistribution efficiency of the steel fibers. The net effect is increased crack propagation and post cracking strength capacity. Improvement in ductility is important because it is a desirable structural property which can provide warning of impending failure.

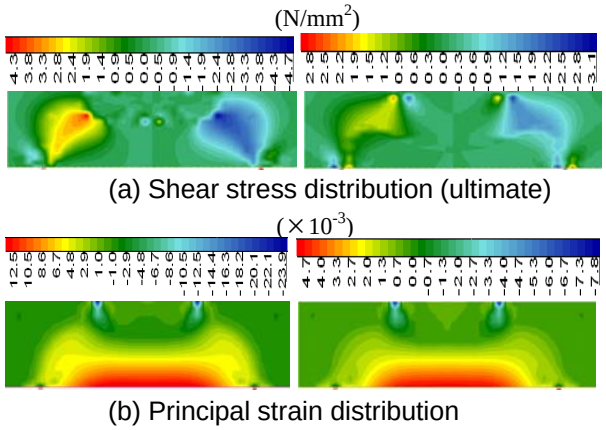

(a) Shear stress distribution (ultimate)

(b) Principal strain distribution

Fig.11 FEM Shear stress and principal strain distribution for a/d=1 group of beams

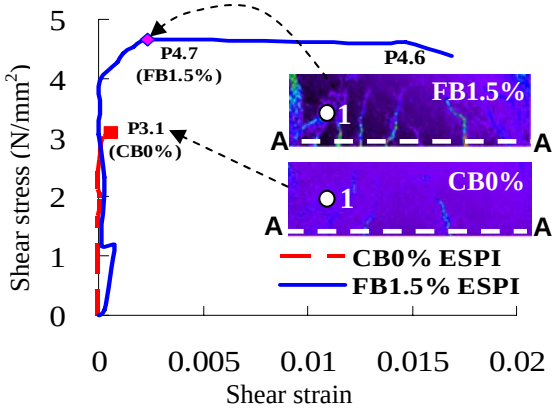

Fig.12 Shear stress-strain curve and strain profile locations for a/d=1 group of beams

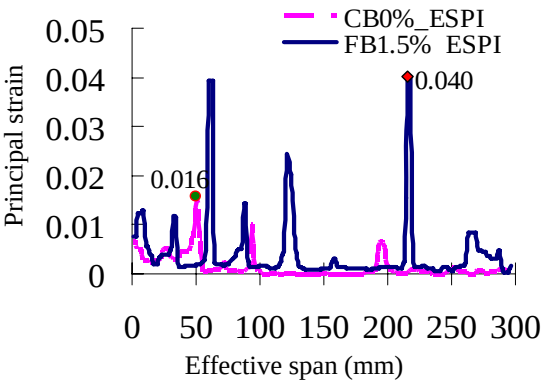

Fig.13 Strain distribution along A-A (Fig.1) for a/d=1 group of beams

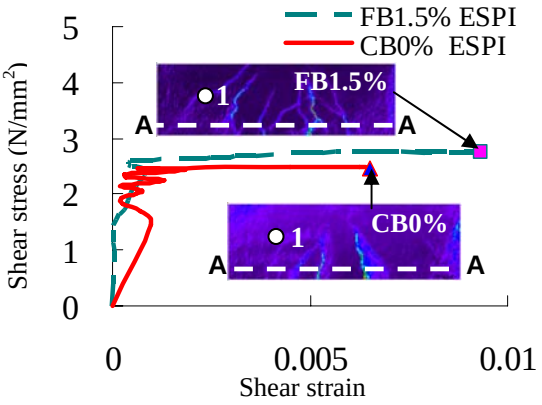

Fig.14 Shear stress-strain curve and strain profile locations for a/d=1.5 group of beams

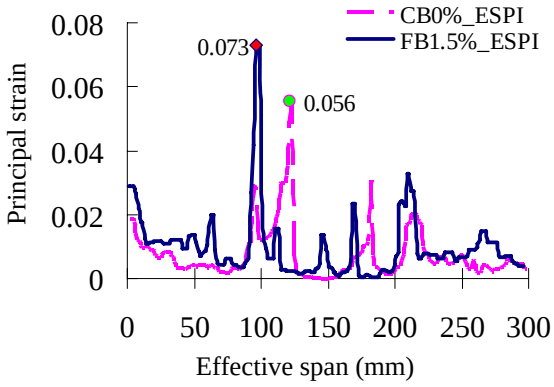

Fig.15 Strain distribution along A-A (Fig.1) for a/d=1.5 group of beams

.

5. CONCLUSIONS

In this study, experimental (optical ESPI) and numerical (FEM) investigation on shear strength and deformation behavior in SFRC beams, subjected to monotonic loading in bending shear were undertaken. The influence of the steel fibers and the effectiveness of the numerical method were examined. From the study, the following principal findings and conclusions are made:

1. Steel fiber reinforced RC beams (FB0.5% to

FB1.5%) showed improved strength and deformation characteristics in comparison with the non fibrous beams (CB0%).

2. Strength, deflection and strain enhancement were found to be effective in fibrous beams failing in shear. SFRC beams with 1.5% steel fibers (FB1.5%) yielded strength increases of 50% and 22% (in both experiments and FEM) in a/d=1 and 1.5 group of beams. The reduction in strength in the latter case is attributed to the flexural-shear failure mode.
3. FB1.5% in a/d=1 group of beams yielded the highest experimental crack strain increase and was found to be 1.5 times that of the control beam (CB0%) in beams.
4. Numerical simulation by FEM reproduced fairly well the experiments. Load deflection curves were in agreement with the experimental result until ultimate failure. Cracking pattern, non linear stress and strain distributions were obtained in which the failure mechanism is illustrated.
5. Use of experimentally derived SFRC stress strain material model was effective in the numerical simulation of the SFRC beams.

ACKNOWLEDGEMENT

This study was supported by Grant-in-Aid for Scientific Research (B19360205) of Japan Society for the Promotion of Science (JSPS). The first author acknowledges the support from Japan Government, Ministry of Education, Culture, Sports, Science and Technology (MEXT). Shinko Kenzai, Ltd. and BASF Pozzolith Ltd. are acknowledged for the supply of the steel fibres and water-reducing agents, respectively. Finally assistance received from Mr.Y.Kosaka, R. Hirahama and H.Nishida is highly appreciated.

REFERENCES

1) Balendra, R.V. et al., “Influence of Steel Fibres on Strength and Ductility of Normal and Light Weight High Strength Concrete,” Elsevier, Building and Environment Journal, No.37, 2001, pp.1361-1367.
2) Rossi P., “Steel Fiber Reinforced Concrete; an Example of French Research,” ACI Materials Journal, Vol.91, 1994, pp. 273-279.
3) Meda, A. and Plizzari, A.G., “New Design Approach for Steel Fiber-Reinforced Concrete Slabs-on-ground Based on Fracture Mechanics,” ACI Structural Journal Vol.101, No. 3, 2004, pp. 298-303.
4) Rao, G.D.T. and Seshu, R.D., “Analytical Model for Torsional Response of Steel Fiber reinforced Concrete Members under Pure Torsion,” Cement and Concrete Composites 27, 2005, pp. 493-501.
5) Minelli, F. and Vicchio, J.F., “Compression Field Modeling of Fiber-Reinforced Concrete members under shear loading,” Vol. 103, No. 2, 2006, pp. 244-252.
6) Calogero, C. et al., “Effectiveness of Stirrups and Steel Fibers as Shear Reinforcements, Cement and Concrete Composites, No.26, pp.777-786, 2004.
7) Casanova, P. et al., “Can Steel Fibers Replace Transverse Reinforcements in Reinforced Concrete Beams?” ACI Journal Vol. 94. No 5, 1997, pp.341-354.
8) Nyomboi, T. et al., “Strength and Deformation Behavior in Normal Steel Fiber Reinforced Concrete by Optical (ESPI) Methods,” Proceedings of the Japan Concrete institute, Vol.30, No.3, 2008, pp. 1489-1494.
9) Feheling, E. and Bullo T., “Ultimate load Capacity of Reinforced Steel Fiber Concrete Deep Beams subjected to Shear”, Proc. of Finite Elements in Civil Engineering Applications, 2002, pp. 209-218.
10) Rots, J.G., “Comparative Study of Crack Models,” Proc. of Finite Elements in Civil Engineering Applications, 2002, pp. 17-27.
11) Tacacks, K.V., “Non Linear Analysis of Prestressed Concrete Beams with a Total Strain Based Model and Full Scale Testing,” Proc. of Finite Elements in Civil Engineering Applications, 2002, pp. 201-208.
12) Matsuda, H. et al., “Non contact and Whole Field Measurement of the Cracking Generation and Development Process of the RC beam by the Speckle Interference Method,” JSCE, Journal of structural Engineering, Vol.52. No.1, 2006, pp. 11-18 (in Japanese).
13) Pallewatta, M.T. et al., “Measurement of Surface Displacement Field of Concrete by Laser Speckle method,” Proceedings of the Japan Concrete institute, 1990, pp. 835-840.
14) JSCE: “Guidelines for Concrete Standard Specification for Concrete Structures, Materials and Construction,” 2002, pp. 76-77.
15) SOFISTIK: “Analysis Programmes,” versions 23. 14.30, 14.16, 13.08, 12.73, 11.16, 11.15. SOFISTIK AG, berschleissheim, CD ROM, 2006.
16) Kutzing L. and Konig G., “Design Principals for Steel Fiber Reinforced Concrete; a Fracture Mechanics Approach,” Lacer No.4, 1999, pp.176-183.
17) Kwak K. et al., “Shear Strength of Steel Fiber-Reinforced Concrete Beams without Stirrups,” ACI Structural Journal No.4, 2002, pp. 530-538.
18) Lim, D.H. and Oh B.H., “Experimental and Theoretical Strength Investigation on Shear of Steel Fiber Reinforced Concrete Beams,” Engineering Structures, No.21, 1999, pp. 937-944.
19) Narayanan R. and Darwish I.Y.S., “Use of Steel Fibers as Shear Reinforcement,” ACI Structural Journal Vol.84, No.3, 1987, pp. 216-227.
20) Yoon-keun K. et al., “Shear strength of steel Fiber Reinforced Concrete Beams without Stirrups,” ACI Structural Journal, Vol.99, No.4, 1999, pp. 282-290.
21) Nyomboi, T. et al., “Stress Strain Relations for Steel Fiber Reinforced Concrete Beams in Shear,” Proc. of International Conference on Applied Mechanics, Durban, S. Africa, 2000, pp. 355 -368.